Dynamic mapping of dengue basic reproduction number

Samuel Benkimoun, Célestine Atyame, Marion Haramboure, Pascal Degenne, Hélène Thébault, Jean-Sébastien Dehecq, Annelise Tran

HAL Id: hal-03342899

https://hal.inrae.fr/hal-03342899

Submitted on 18 Oct 2021

Dynamic mapping of dengue basic reproduction number

Samuel Benkimoun [a,b,g,h,*], Célestine Atyame [c], Marion Haramboure [a,b,d,e], Pascal Degenne [d,e], Hélène Thébault [f], Jean-Sébastien Dehecq [f], Annelise Tran [a,b,d,e]

[a] CIRAD, UMR ASTRE, F-97490 Sainte-Clotilde, La Réunion, France
[b] ASTRE, Univ Montpellier, CIRAD, INRAE, Montpellier, France
[c] Université de la Réunion, UMR PIMIT, F-97490 Sainte-Clotilde, La Réunion, France
[d] CIRAD, UMR TETIS, F-34398 Montpellier, France
[e] TETIS, Univ Montpellier, AgroParisTech, CIRAD, CNRS, INRAE, Montpellier, France
[f] Agence Régionale de Santé, F-97490 Sainte-Clotilde, La Réunion, France
[g] Géographie-Cités, UMR 8504, Université Paris 1, France
[h] Centre de Sciences Humaines, UMIFRE 20, CNRS-MEAE, India

ARTICLE INFO

ABSTRACT

We developed a method to produce time-varying maps for dengue transmission risk, using the Ross-Macdonald framework and differential equations to estimate spatially the basic reproduction number (R_0) of a vector-borne disease. The components of the R_0 formula were derived partly from a mosquito population dynamics model integrating meteorological and environmental variables, and partly from temperature-dependent functions of vector competence and the extrinsic incubation period. The method was applied on Reunion Island, a tropical island located in the Indian Ocean, where the mosquito *Aedes (Stegomyia) albopictus* has been responsible for large and numerous outbreaks of dengue. As a validation, predicted maps and dynamic outputs were compared with the distribution of confirmed dengue cases registered during the year 2018 in Reunion Island. The results highlight strong agreements between the observed epidemiological patterns and predicted R_0 distribution and temporal dynamics. This finding demonstrates the relevance and efficiency of the spatialised basic reproduction number (R_0) to develop an operational dynamic mapping tool for dengue surveillance and control. The resulting method could be of great use in a health policy-making context, providing a time and space awareness to the dengue risk perception.

Introduction

Vector-borne diseases (VBD) are caused by pathogens – parasites, bacteria, or viruses, whose transmission between vertebrate hosts requires a hematophagous arthropod. According to the World Health Organization, they account for more than 17% of infectious diseases, causing 700,000 deaths annually [1]. Among them, mosquito-borne diseases such as malaria and dengue place a high burden on the impacted countries and their health systems, mainly in tropical and subtropical areas. The high diversity of species involved in the transmission of mosquito-borne pathogens increases the occurrence of these diseases in both rural and environments [2–4]. In the absence of effective vaccines and specific treatments, vector control is the only measure to interrupt the transmission of vector-borne pathogens. Therefore, the capacity to predict periods and locations at risk of disease transmission

would help improve vector control measures, with better-measured impacts. Moreover, mapping the epidemic risks is an essential step to further orientate health policies for sensitization campaigns of human populations [5].

Modelling of vector-borne diseases, including process-based and empirical approaches, has a long and rich history [6–9,52]. Most mathematical models use the theoretical framework developed for malaria by Ross and Macdonald [10,11]. Indeed, such a framework allowed a simple formulation of the basic reproduction number (R_0) of a vector-borne disease. This reproduction number can be understood in the following way: it is the expected number of hosts that would become infected from the introduction of a single infected host in a fully susceptible population, as a function of entomological and epidemiological parameters (vector biting rate, mortality rate, competence and extrinsic incubation period, vector-to-host ratio, transmission probability,

---

duration of infectiousness in hosts) [10,12]. R_0 has become a key notion in mathematical epidemiology as $R_0 = 1$ is considered as the epidemic threshold that predicts whether a disease will spread at the onset of the epidemic [13].

As arthropods' life cycle is very much driven by climatic and environmental determinants, this latter also strongly impacts the transmission of vector-borne diseases, which may vary in space and time. Thus, methods have been developed to map R_0 for vector-borne diseases from environmental and meteorological variables as predictors [14]. For example, seasonal R_0 maps accounting for meteorological variables were produced at a national level for bluetongue [14], and maps at continental scale were used to better understand and predict the impact of climate change on the risk of bluetongue in Europe [15]. Recently, R_0 maps of malaria were produced at a regional scale in Greece, integrating meteorological variables as well as entomological, environmental, and social data [16].

Yet, as far as we know this R_0 mapping approach has not been used so far for arthropod-borne viruses (arboviruses) transmitted by *Aedes* mosquitoes. In particular, it was not applied to dengue fever, the most prevalent arboviral infection, endemic in more than 100 countries, including Reunion Island, and responsible for 390 million infections estimated annually [17]. A wide variety of predictors and modelling approaches have been used either to create dengue risk maps [18] or estimate R_0 values [12,19–21] but to our knowledge, both approaches have never been combined. A recent study provided a framework for mapping dengue spatially time-varying reproductive numbers from reported cases locations [22], but such approach does not account for meteorological and environmental drivers (*i.e.* vegetation, urbanization type, etc.) that could impact spatial and temporal vector abundances, thus resulting in heterogeneities in virus transmission.

In this study, we aimed to produce time-varying dengue R_0 maps in Reunion Island, a tropical island located in the Indian Ocean, where the mosquito *Aedes (Stegomyia) albopictus* is responsible for a current large outbreak of dengue [23]. As highly heterogeneous vector densities have been reported in the island [24], a rainfall- and temperature-driven model of *Ae. albopictus* populations ('ALBORUN') was recently developed to predict vector abundance at a local scale, accounting for variations in the availability of breeding sites [25]. We used the 'ALBORUN' model and the Ross-Macdonald framework to derive dynamic dengue R_0 maps from meteorological and environmental variables, and assessed the relevance of such an approach by comparing the predicted maps and dynamics with the number of confirmed dengue cases registered during the year 2018.

Material and methods

Study area. Reunion Island (2500 km^2 and 865,826 inhabitants in 2018) is a French overseas territory located in the south-western Indian Ocean (Fig. 1). Its subtropical climate with mild austral winters (May-October) and warm austral summers (November-April) is suitable for the development of *Aedes albopictus* mosquitoes throughout the year [24,25] local variations of climate are important due to a highly uneven relief and different wind exposures.

Arboviruses are a recurring public health issue on Reunion Island, with a massive dengue epidemic in 1977 that affected up to 35% of the population [26]. In 2005, a chikungunya epidemic again reached 35% of the island residents [27]. After several years of moderate virus circulation, a large dengue outbreak started in 2018, with 28,141 cases reported between January 2018 and April 2020 [28].

Human population data. 2016 census data were obtained at IRIS ("Ilots regroupés pour l'information statistique") level (https://www.insee.fr/fr/statistiques/4228434). Those sub-urban units correspond to the most detailed level of population census available in Reunion (n = 344) (Fig. 1). The population was then estimated at the scale of the operational zones mapping used by the local vector control services (n = 1203). To scale down from the IRIS level of the French census, built-up
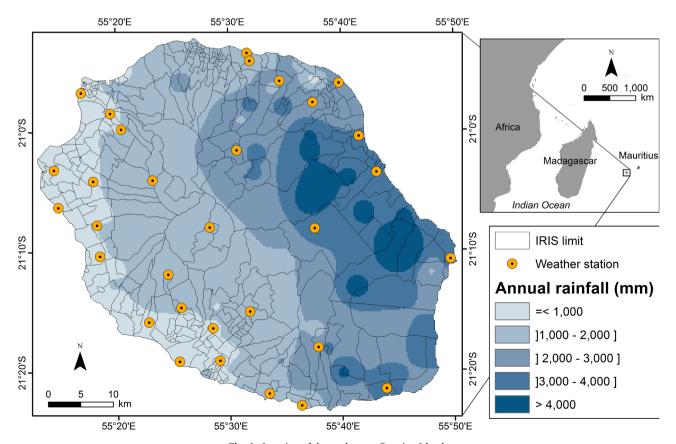

Fig. 1. Location of the study area, Reunion Island.

spatial data were downloaded from the French National Geographic Institute (https://data.geocatalogue.fr/id/dataset/a51dafeb-bd2a-4b8 a-929b-ca539a44217e) and the population was reallocated at the pro-rata of the houses within the operational zones, as compared to the total number of houses in the intersected IRIS zones. Geographic Information System spatial analysis functions were used (QGIS 3.4). Only operational zones located in residential areas with an estimated population greater than 10 (*i.e.*, excluding administrative, business, or sparse habitat) were selected for R_0 computation (n = 1189).

Epidemiological data. The weekly confirmed dengue cases recorded in 2018 were aggregated at the IRIS level. The incidence rate (number of confirmed cases in 2018 per 10,000 inhabitants) per IRIS was calculated using 2016 census data.

Meteorological data. We obtained daily mean temperature and rainfall recorded from 2017 to 2018 at 32 weather stations (Fig. 1) from the national meteorological service 'Meteo France' (https://publitheque .meteo.fr). Indeed, the acquisition of meteorological data covering the year before the period of interest (2018) was necessary for the initialization of the mosquito population dynamics model [25].

'ALBORUN' population dynamics model. This process-based model of *Ae. albopictus* population dynamics on Reunion Island is based on a system of ordinary differential equations (ODE) [53,54] that represents all steps of the mosquito life cycle, considering aquatic juvenile and aerial female adult stages (Fig. 2) [25] (https://doi. org/10.18167/DVN1/XF2I3L). Transition functions from one stage to the next and mortality rates are driven by daily rainfall and temperature. The model inputs are *i)* the operational zones used by the vector control service, characterized by their standard fixed and variable environment carrying capacities, two values describing the availability and characteristics of the mosquito breeding sites in the zone (based on field observations, see [25] for details), *ii)* the location of weather stations, and *iii)* the corresponding daily rainfall and temperature. As output, 'ALBORUN' predicts the abundances of *Ae. albopictus* mosquitoes per stage at a weekly frequency, and for each operational zone for which the rainfall and temperature values from the closest weather station are simply attributed.

The following parameters, functions, and outputs are used for the R_0 model (see below): the daily transition rate from host-seeking to engorged adults (γ_{Ah}), the mortality rate of adult mosquitoes (m_A), the mortality rate related to seeking behaviour (μ_r), the number of host-seeking female mosquitoes (A_h) and the total number of *Ae. albopictus* female mosquitoes (A_{tot}).

R_0 model. We used the classic computation of R_0 from the vectorial capacity (V), which estimates the daily number of new vector infectious bites that arises from one infected host introduced into an entirely susceptible host population [29,30]:

$$V = \frac{ma^2p^n}{-ln(p)} \tag{1}$$

where m is the vector density per host, a a daily biting rate, p the daily survival rate, n the duration of the extrinsic incubation period (EIP).

The basic reproduction number R_0 is obtained by multiplying V by the vector competence (b) and the duration of host viremia ($1/r$, where r is the host recovery rate):

$$R_0 = \frac{V}{r}.b \tag{2}$$

With the exception of r, all components of this R_0 formula (Eqs. (1) and (2)) were considered space- and time-dependent. Moreover, in absence of the genetic structure of *Ae. albopictus* populations in Reunion Island [31], meteorological and environmental factors were considered the main drivers of the vector competence and the vectorial capacity. Most components of the vectorial capacity (Eq. (1)), namely m, a, and p the daily survival rate, were derived from the 'ALBORUN' model for each operational zone and each time step (Table 1). The EIP (n) and the vector competence (b) were defined as functions of temperature varying over time. Polynomial regressions adjusted to experimental values [32] were used to express the relationship between the temperature and EIP and vector competence (Table 1), regarding the dengue virus serotype 2 (DENV-2), the serotype circulating in Reunion Island in 2018 [23]. The impact of dengue infection on the mosquitoes' life cycle, very uncertain [33], has been neglected, as well as an eventual variation between symptomatic and asymptomatic hosts regarding incubation period and viremia.

Simulations. The R_0 model was implemented in *Ocelet* language

Table 1
Estimation of dengue R_0 parameters, Reunion Island.

Notation	Definition*	Expression*	Reference
m	Vector density per host	$\frac{A_{tot}}{H}$	[25,49]
a	Daily biting rate	$\frac{A_h}{A_{tot}}.\gamma_{Ah}, with \gamma_{Ah} = 0.2$	[25]
p	Daily survival rate	$1 - m_A - \frac{A_{2h}+A_{2o}}{A_{tot}}.\mu_r, with \mu_r = 0.08$	[25]
n	EIP	$0.11T^2 - 7.13T + 121.17$	[32]
b	Vector competence	$-0.0043T^2 + 0.2593T - 3.2705$	[32]
r	Host recovery rate	0.2	[50]

*T temperature; H: human population; A_{tot}: total number of *Ae. albopictus* female mosquitoes A_h: number of *Ae. albopictus* host-seeking females; γ_{Ah}: daily transition rate from host-seeking to engorged adults; m_A: mortality rate of adult mosquitoes; μ_r: mortality rate related to seeking behavior. A_{tot}, A_h, A_{2h}, A_{2o} and m_A are estimated by 'ALBORUN' model (see [25] for details).
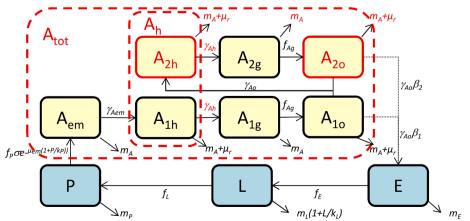

Fig. 2. Diagram of the *Aedes albopictus* population dynamics model (ALBORUN). The model predictions focus on the sole female mosquito population, being the one that bites. In blue, the aquatic stages (*E*: eggs; *L*: larvae; *P*: pupae); in yellow the female adult stages (*A_em*: emerging; *A_1*: nulliparous, *A_2*: parous, *A_tot*: total; *h*: host-seeking; *g*: resting; *o*: ovipositing). Parameters (greek letters) are constant, functions (latin letters) are weather-driven functions, varying over time. For stage *X*, γ_X and f_X are transition rates to the next stage; μ_X and m_X mortality rates; β_X is the egg laying rate; σ is the sex-ratio at the emergence; μ_r is an additional adult mortality rate related to seeking behavior; k_X the environment carrying capacity. Stages, parameters and functions values used for R_0 computation are red highlighted. (For interpretation of the references to colour in this figure legend, the reader is referred to the web version of this article.)

(www.ocelet.org), by adapting the 'ALBORUN' mosquito population model (https://doi.org/10.18167/DVN1/XF2I3L), extended by a module of R_0 calculation. R_0 values are then computed for each operational zone from dynamically updated values of the different components of the vectorial capacity at each time step (Eqs. (1) and (2)). Simulations were run over two years (2017–2018) because the first year was not retained for output computation.

Evaluation of the R_0 model. The capacity of the R_0 model to predict the spatial distribution of dengue transmission risk was assessed by comparing the annual statistics (mean and maximum values) of simulated R_0 with the number of confirmed dengue cases reported, at the IRIS level. On the other hand, the capacity of the R_0 model to predict the seasonal variations of dengue transmission throughout the year was assessed by comparing for each week w, the weekly R_0 median value, with the ratio n_w/n_{w-1} between the numbers of confirmed dengue cases reported during week w and the precedent week ($w-1$), using Pearson correlation coefficient.
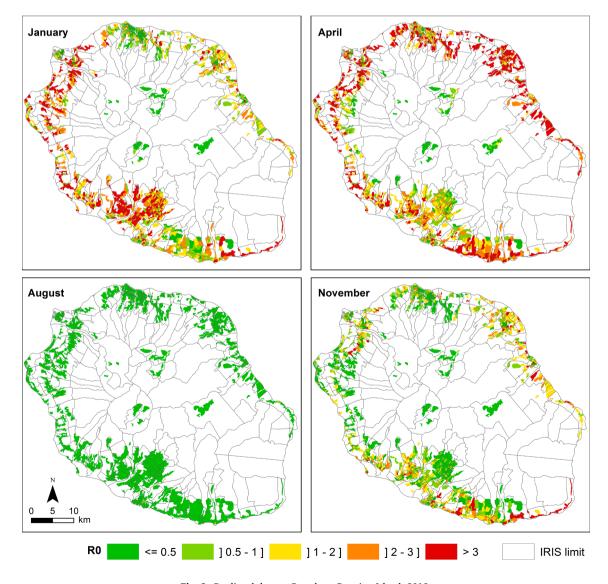
Results

Dengue R_0 maps highlight spatial and seasonal variations of the risk of dengue transmission in Reunion Island. For each operational zone defined by the vector control services (mean surface of 33 ha), our model predicts dengue R_0 value at a weekly frequency. The resulting maps highlight high spatial and seasonal variations on Reunion Island (Fig. 3, Video file 1). Higher R_0 values are predicted during the austral summer (January-April), and in western and southern coastal areas (Fig. 3). When R_0 peaks, almost all regions of the islands are at risk ($R_0 > 1$), except the inner mountainous zones (*e.g.* April, Fig. 3). During the austral winter, R_0 drops below the threshold value of one in all regions (*e.g.* August, Fig. 3). At the beginning of the hot and wet season (November) R_0 values start increasing, mostly in the southern part of the island (Fig. 3). Spatio-temporal dynamics of the R_0 components, vectorial capacity, extrinsic incubation period, and vector competence, are provided in Supplementary Fig. S1-3.

The spatial distribution of predicted R_0 is significantly correlated with dengue incidence.

Significant correlations were found between annual maximum R_0 values computed at IRIS level (Fig. 4A) and dengue incidence (Fig. 4B) (Pearson r = 0.41, p < 10^{-12}). The correlation with the mean R_0 values was also significant (Pearson r = 0.30, p $\langle 10^{-6} \rangle$). The map of the annual maximum of R_0 values computed at IRIS level highlights several areas with high predicted R_0, mainly located on the western coast of the island (Fig. 4A).

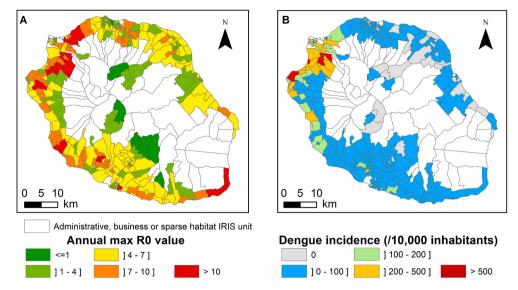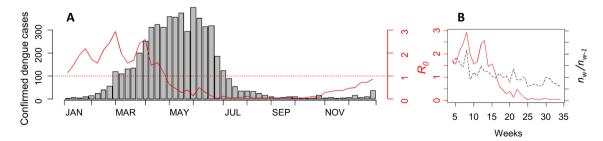**Fig. 3.** Predicted dengue R_0 values, Reunion Island, 2018.

Fig. 4. Predicted R_0 and observed incidence for dengue, Reunion Island, 2018. A) Predicted annual maximum R_0 value computed at IRIS level. B) Dengue incidence on Reunion Island, 2018.

Seasonal dynamics of predicted dengue R_0 correlates with the temporal dynamics of dengue transmission. According to our model, the predicted median R_0 value on Reunion Island was over the threshold of one from January to May 2018 (Fig. 5A). It started decreasing at the beginning of April. During this period, the number of confirmed dengue cases on the island steadily increased. It is important to look at the moment where the R_0 crosses the 1 threshold, meaning a decrease in the transmission dynamic of the virus. In our model, it happens during the first week of May. Comparing this to the actual numbers of 2018 shows that a plateau is reached at this very same time. The number of recorded cases is stabilizing at its highest level for about a month (showing a comprehensible delay of a couple of weeks in the effect of this R_0 decrease, due to the incubation period of previously infected individuals for example). Then, the number of cases dropped at the beginning of the austral winter (end of June), when the median R_0 reaches its minimum value ($R_0 = 0.03$, week 25: June 17th). Very low R_0 values were predicted between July and November; R_0 started increasing again at the end of October (Fig. 5A). The variation of weekly R_0 median values could be compared with the ratio n_w/n_{w-1} for the period with n greater than 10, *i.e.* between weeks 5 (January 28th) and 35 (August 28th) (Fig. 5B), depicting an even clearer adequation between the model outputs and the outbreak. The comparison between the two indices showed a strong and significant correlation (Pearson r = 0.77, p < 10^{-6}), and their respective drop below the value of 1 appears synchronized.

Discussion

In this study, we used the Ross and Macdonald framework [11] to propose a real-time mapping method of the basic reproduction number of dengue fever from the weather (rainfall and temperature) and environmental variables (availability and characteristics of the *Ae. albopictus* breeding sites). Predicted R_0 values were compared with 2018 dengue outbreak data from Reunion Island at fine spatial and temporal scales [23]. It is important to reassert that the model was at no point calibrated to specifically fit this data; instead, parameters and functions were defined based on the results of previous experimental and observational studies thus combining all current knowledge on the ecological mechanisms. Our results demonstrate the efficiency of such an approach to develop an operational dynamic mapping tool for dengue surveillance and control, potentially useful for decision-makers. The dengue R_0 module was implemented in the 'ALBORUN' tool, which is routinely used by the Health Regional Agency in Reunion Island [25].

Spatial patterns of dengue R_0 in Reunion Island. According to our results, R_0 values computed at the IRIS level ranged from 0 to 14.85 (mean: 5.12) (Fig. 4A), which is consistent with dengue R_0 estimations in other tropical countries [12]. Higher values of estimated dengue R_0 are predicted in the western and southern regions (Figs. 3 and 4A): in these leeward coastal areas, temperatures are warmer than in other parts of the island, favouring dengue transmission with shortened extrinsic incubation period and increased vector capacity (Supplementary Figs. S1 and S2). Moreover, although the rainfall is lower in these areas, densities of *Ae. albopictus* populations are higher as compared to other

Fig. 5. A) Predicted median R_0 values dynamics (red line) and dengue confirmed cases (grey bars), Reunion Island, 2018. The red dotted line indicates the threshold of one. B) Predicted median R_0 values dynamics (red line) and ratio n_w/n_{w-1} (dashed black line) between the numbers of confirmed dengue cases reported during week w and during the precedent week $w-1$, Reunion Island, 2018, weeks 5 (January 28th) to 35 (August 28th). (For interpretation of the references to colour in this figure legend, the reader is referred to the web version of this article.)

areas, due to human-made oviposition sites such as flower plates, pots, or barrels that remain available over time in urban and peri-urban neighbourhoods [25,34]. Interestingly, the differences in vector competence between *Ae. albopictus* populations from the eastern and western coasts (Supplementary Fig. S3) are less marked than those predicted with EIP (Supplementary Fig S2) and vectorial capacity (Supplementary Fig. S1), suggesting that in Reunion Island, the spatial heterogeneity of dengue predicted R_0 is mostly driven by vector ecology rather than molecular interactions between *Ae. albopictus* populations and dengue viruses. This result corroborates the conclusions of previous modelling and experimental studies on *Ae. albopictus* competence for dengue virus transmission, and on the importance of the presence of breeding sites to support the transmission [32,35,36] and endemicity of dengue in tropical areas [37].

Predicted dengue R_0 values computed at IRIS level were significantly correlated with dengue incidence, suggesting that the resulting R_0 maps (Figs. 3 and 4A) could be used to identify areas at risk for virus transmission. Our results thus stress that most of those areas are located on the western and southern coasts (Fig. 4A). Of note, areas with high R_0 predicted values do not fully overlap those with high observed dengue incidence, and overall, the R_0 index trends to overestimate the risk of dengue: it is the case for example in the southern and eastern coasts, where few dengue cases were reported in 2018 in areas with high predicted R_0 values (Fig. 4). Several non-exclusive assumptions may explain these discrepancies. Firstly, a large number of paucisymptomatic cases may remain undetected by the surveillance system [38]. Secondly, by definition R_0 reveals the number of secondary cases arising from the introduction of a single case in a susceptible population, but it does not capture the risk of introduction, which is related to human mobility. Thus, a low number of cases may be reported in areas with high R_0 values but poorly connected to other regions of the island in terms of human population flows, for example, south-eastern areas (Supplementary Fig. S4). Thirdly, in R_0 computation the human population was assumed fully susceptible to dengue serotype 2, which may not be the case. An estimation of the real reproduction number R, taking into account the population immunity, would improve the model. Lastly, the vector control measures which are implemented when a dengue case is reported in a zone [23] can substantially reduce the virus transmission and the number of secondary cases, if promptly detected. This effect could be considered by the model in future investigations.

Dynamics of dengue R_0 in Reunion Island. Our analysis highlighted R_0 variations over time in relation to temperature and rainfall: predicted R_0 values were over the threshold of one during the hot and rainy season, and below the threshold during the austral winter, mainly due to colder and potentially lethal temperatures for mosquito populations. R_0 starts increasing again in November, at the beginning of the austral summer (Fig. 5A). This result is in keeping with the seasonal pattern described in other tropical areas from observational and modelling studies [39–42]. The predicted variations of R_0 are also consistent with the dynamics of dengue epidemics observed on Reunion Island (Fig. 5A): the number of cases increases steadily from January to May, when R_0 is greater than one, and strongly decreases at the end of June when R_0 reaches its minimum. The strong and significant correlation of R_0 with the ratio n_w/n_{w-1}, an index depicting the variation of the number of cases on a weekly basis (Fig. 5B), suggests that predicted R_0 could be used to identify periods at risk for virus transmission.

Limitations and perspectives. The method proposed in this study has the advantage of simplicity and parsimony (Eqs (1) and (2)). The mechanist model behind those results has also been applied to other territories [51] and gave similarly consistent outputs regarding the vector ecology, which tends to drive away the eventuality of an over-fit. The comparison with the dengue cases reported in Reunion Island in 2018 proves its efficiency as a dynamic mapping tool for dengue surveillance and control, which would be relevant to orientate further health policies. However, different weather-driven processes were not taken into account in our model, such as the impact of diurnal thermal

range on vector competence [30] or a temperature-dependent host-vector transmission rate [43]. The inclusion of such processes could improve this first R_0 model. Moreover, as above-mentioned, by construction R_0 does not capture the risk of the introduction of an index case in an area. A model including both importation risk estimates, from human mobility (Supplementary Fig. S4), and onward transmission [44] could be used to improve the predictions.

DENV2-serotype was the only serotype circulating on Reunion Island in 2018 [23], thus in this study R_0 functions (Table 1) were defined for this particular serotype. To assess the risk of transmission of the three other dengue serotypes in Reunion Island, the functions would need to be modified as vector competence and the extrinsic incubation period can change according to the dengue virus serotype involved in the transmission [45]. Indeed, DENV-1, DENV-3, and DENV-4 serotypes have been reported on the island in recent years and an autochthonous circulation of these three serotypes has been reported in 2020. Moreover, with time the immunity will increase and therefore the population could not be considered as fully susceptible: the cartography of the dengue reproduction rate (R), with a formula taking into account the immunity of the human population, would be more appropriate in the future. Another perspective would be to account for the vector control actions (fumigation of mosquito adults, cleaning the water-holding containers that serve as breeding sites for *Ae. albopictus*) in order to simulate *in silico* different scenarios of control strategies, and study their impact on the reduction of R_0. Finally, the approach developed in this work could be applied to other pathogens transmitted by *Ae. albopictus,* such as the Chikungunya virus, which caused a very severe outbreak in Reunion Island in 2006, and the Zika virus, which recently spread worldwide and constitutes a threat for Reunion Island. Moreover, as the mosquito population dynamics model framework has already been used for other geographical contexts [46] and/or mosquito species [47,48], our model also offers some broad transposition possibilities by adapting the parameters from the existing scientific literature.

Conclusion

In this paper, we presented an original method coupling a mechanistic mosquito population dynamics model with the Ross-Macdonald R_0 formula to evaluate risks with regard to mosquito-borne diseases. This model operates at a very fine spatial scale, adapted to vector surveillance and control interventions, and on a weekly frequency. This strong reactivity to spatial and temporal trends makes the model a reliable tool for health policymakers to implement effective public health policies against dengue. The proposed framework could be deployed in other and various geographical and epidemiological contexts.

Ethics statements

Dengue cases are reported to the regional health agency to conduct vector control measures. As data from an epidemiological record, institutional review and informed consent were not required. All data analyzed were anonymized.

Data Availability statement

ALBORUN code is available from CIRAD dataverse https://doi.org/10.18167/DVN1/XF2I3L

Authors' contributions

SB contributed to the acquisition and preparation, modelling, analysis and interpretation of data and helped draft the manuscript. CA contributed to analysis and interpretation of data and critically revised the manuscript. MH and PD contributed to modelling, analysis and interpretation of data and critically revised the manuscript. HT and JSD conceived of the study, contributed to the acquisition and interpretation

of data, and revised the manuscript. AT conceived of the study, designed the study, contributed to modelling, analysis and interpretation of data and drafted the manuscript. All authors gave final approval for publication and agreed to be held accountable for the work performed therein.

Declaration of Competing Interest

The authors declare that they have no known competing financial interests or personal relationships that could have appeared to influence the work reported in this paper.

Acknowledgments

Appendix A. Supplementary data

Supplementary data to this article can be found online at https://doi. org/10.1016/j.rinp.2021.104687.

References

[1] WHO. 2020 Vector-borne diseases - Key facts. https://www.who.int/news-room/f act-sheets/detail/vector-borne-diseases.

[2] Cox J, Grillet ME, Ramos OM, Amador M, Barrera R. Habitat segregation of dengue vectors along an urban environmental gradient. Am J Tropical Med Hygiene 2007; 76:820–6. https://doi.org/10.4269/ajtmh.2007.76.820.

[3] Harrington LC, Scott TW, Lerdthusnee K, Coleman RC, Costero A, Clark GG, et al. Dispersal of the dengue vector Aedes aegypti within and between rural communities. Am J Tropical Med Hygiene 2005;72:209–20.

[4] Vazquez-Prokopec GM, Kitron U, Montgomery B, Horne P, Ritchie SA. Quantifying the spatial dimension of dengue virus epidemic spread within a tropical urban environment. PLoS Neglected Tropical Dis 2010;4:e920. https://doi.org/10.1371/ journal.pntd.0000920.

[5] Ouedraogo S, Benmarhnia T, Bonnet E, Some PA, Barro AS, Kafando Y, Soma DD, Dabire RK, Sare D, Fournet F, et al. Evaluation of effectiveness of a community-based intervention for control of dengue virus vector, Ouagadougou, Burkina Faso. Emerging Infectious Dis 2018;24:1859–67. https://doi.org/10.3201/ eid2410.180069.

[6] Reiner Jr RC, Perkins TA, Barker CM, Niu T, Chaves LF, Ellis AM, George DB, Le Menach A, Pulliam JR, Bisanzio D, et al. A systematic review of mathematical models of mosquito-borne pathogen transmission: 1970-2010. J R Society, Interface 2013;10:20120921. https://doi.org/10.1098/rsif.2012.0921.

[7] Smith DL, Perkins TA, Reiner Jr RC, Barker CM, Niu T, Chaves LF, Ellis AM, George DB, Le Menach A, Pulliam JR, et al. Recasting the theory of mosquito-borne pathogen transmission dynamics and control. Trans R Society Tropical Med Hygiene 2014;108:185–97. https://doi.org/10.1093/trstmh/tru026.

[8] Sadeghieh T, Waddell LA, Ng V, Hall A, Sargeant J. A scoping review of importation and predictive models related to vector-borne diseases, pathogens, reservoirs, or vectors (1999-2016). PloS one 2020;15:e0227678. https://doi.org/ 10.1371/journal.pone.0227678.

[9] Rogers DJ. Models for vectors and vector-borne diseases. Adv Parasitol 2006;62: 1–35. https://doi.org/10.1016/S0065-308X(05)62001-5.

[10] Macdonald G. The epidemiology and control of malaria. Oxford, UK: Oxford University Press; 1957.

[11] Smith DL, Battle KE, Hay SI, Barker CM, Scott TW, McKenzie FE. Ross, Macdonald, and a theory for the dynamics and control of mosquito-transmitted pathogens. PLoS Pathogens 2012;8:e1002588. https://doi.org/10.1371/journal. ppat.1002588.

[12] Liu Y, Lillepold K, Semenza JC, Tozan Y, Quam MBM, Rocklov J. Reviewing estimates of the basic reproduction number for dengue, Zika and chikungunya across global climate zones. Environ Res 2020;182:109114. https://doi.org/ 10.1016/j.envres.2020.109114.

[13] Heffernan JM, Smith RJ, Wahl LM. Perspectives on the basic reproductive ratio. J R Society, Interface 2005;2:281–93. https://doi.org/10.1098/rsif.2005.0042.

[14] Hartemink NA, Purse BV, Meiswinkel R, Brown HE, de Koeijer A, Elbers AR, et al. Mapping the basic reproduction number (R(0)) for vector-borne diseases: a case study on bluetongue virus. Epidemics 2009;1:153–61. https://doi.org/10.1016/j. epidem.2009.05.004.

[15] Guis H, Caminade C, Calvete C, Morse AP, Tran A, Baylis M. Modelling the effects of past and future climate on the risk of bluetongue emergence in Europe. J R Soc Interface 2012;9:339–50. https://doi.org/10.1098/rsif.2011.0255.

[16] Pergantas P, Tsatsaris A, Malesios C, Kriparakou G, Demiris N, Tselentis Y. A spatial predictive model for malaria resurgence in central Greece integrating entomological, environmental and social data. PLoS ONE 2017;12:e0178836. https://doi.org/10.1371/journal.pone.0178836.

[17] WHO. 2020 Dengue and severe dengue - Key facts. https://www.who.int/news -room/fact-sheets/detail/dengue-and-severe-dengue.

[18] Louis VR, Phalkey R, Horstick O, Ratanawong P, Wilder-Smith A, Tozan Y, et al. Modeling tools for dengue risk mapping - a systematic review. Int J Health Geographics 2014;13:50. https://doi.org/10.1186/1476-072X-13-50.

[19] Andraud M, Hens N, Marais C, Beutels P. Dynamic epidemiological models for dengue transmission: a systematic review of structural approaches. PLoS ONE 2012;7:e49085. https://doi.org/10.1371/journal.pone.0049085.

[20] Johansson MA, Hombach J, Cummings DA. Models of the impact of dengue vaccines: a review of current research and potential approaches. Vaccine. 2011;29: 5860–8. https://doi.org/10.1016/j.vaccine.2011.06.042.

[21] Favier C, Degallier N, Rosa-Freitas MG, Boulanger JP, Costa Lima JR, Luitgards-Moura JF, et al. Early determination of the reproductive number for vector-borne diseases: the case of dengue in Brazil. Trop Med Int Health 2006;11:332–40. https://doi.org/10.1111/j.1365-3156.2006.01560.x.

[22] Ng TC, Wen TH. Spatially adjusted time-varying reproductive numbers: understanding the geographical expansion of urban dengue outbreaks. Sci Rep 2019;9:19172. https://doi.org/10.1038/s41598-019-55574-0.

[23] Vincent M, Larrieu S, Vilain P, Etienne A, Solet JL, Francois C, et al. From the threat to the large outbreak: dengue on Reunion Island, 2015 to 2018. Euro Surveillance 2019;24. https://doi.org/10.2807/1560-7917. ES.2019.24.47.1900346.

[24] Boyer S, Foray C, Dehecq JS. Spatial and temporal heterogeneities of Aedes albopictus density in La Reunion Island: rise and weakness of entomological indices. PLoS ONE 2014;9:e91170. https://doi.org/10.1371/journal.pone.0091170.

[25] Tran A, Mangeas M, Demarchi M, Roux E, Degenne P, Haramboure M, et al. Complementarity of empirical and process-based approaches to modelling mosquito population dynamics with Aedes albopictus as an example-Application to the development of an operational mapping tool of vector populations. PLoS ONE 2020;15:e0227407. https://doi.org/10.1371/journal.pone.0227407.

[26] Paupy C, Girod R, Salvan M, Rodhain F, Failloux AB. Population structure of Aedes albopictus from La Reunion Island (Indian Ocean) with respect to susceptibility to a dengue virus. Heredity 2001;87:273–83. https://doi.org/10.1046/j.1365-2540.2001.00866.x.

[27] Renault P, Solet JL, Sissoko D, Balleydier E, Larrieu S, Filleul L, et al. A major epidemic of chikungunya virus infection on Reunion Island, France, 2005–2006. Am J Tropical Med Hygiene 2007;77:727–31.

[28] Santé Publique France. Surveillance de la dengue à la Réunion. Point au avril 2020. Saint Denis, Ile de la Réunion: Santé Publique France 2020. https://www.sante publiquefrance.fr/content/download/249785/2591537.

[29] Garrett-Jones C. Prognosis for Interruption of Malaria Transmission through Assessment of the Mosquito's Vectorial Capacity. Nature 1964;204:1173–5. https://doi.org/10.1038/2041173a0.

[30] Lambrechts L, Paaijmans KP, Fansiri T, Carrington LB, Kramer LD, Thomas MB, et al. Impact of daily temperature fluctuations on dengue virus transmission by Aedes aegypti. PNAS 2011;108:7460–5. https://doi.org/10.1073/ pnas.1101377108.

[31] Latreille AC, Milesi P, Magalon H, Mavingui P, Atyame CM. High genetic diversity but no geographical structure of Aedes albopictus populations in Reunion Island. Parasites Vectors 2019;12:597. https://doi.org/10.1186/s13071-019-3840-x.

[32] Guo XX, Zhu XJ, Li CX, Dong YD, Zhang YM, Xing D, et al. Vector competence of Aedes albopictus and Aedes aegypti (Diptera: Culicidae) for DEN2-43 and New Guinea C virus strains of dengue 2 virus. Acta Trop 2013;128:566–70. https://doi. org/10.1016/j.actatropica.2013.08.006.

[33] Lambrechts L, Failloux AB. Vector biology prospects in dengue research. Mem Inst Oswaldo Cruz 2012;107:1080–2. https://doi.org/10.1590/s0074-02762012000800022.

[34] Delatte H, Dehecq JS, Thiria J, Domerg C, Paupy C, Fontenille D. Geographic distribution and developmental sites of Aedes albopictus (Diptera: Culicidae) during a Chikungunya epidemic event. Vector Borne Zoonotic Dis 2008;8:25–34. https:// doi.org/10.1089/vbz.2007.0649.

[35] Brady OJ, Golding N, Pigott DM, Kraemer MU, Messina JP, Reiner Jr RC, Scott TW, Smith DL, Gething PW, Hay SI. Global temperature constraints on Aedes aegypti and Ae. albopictus persistence and competence for dengue virus transmission. Parasites Vectors 2014;7:338. https://doi.org/10.1186/1756-3305-7-338.

[36] Vazeille M, Mousson L, Rakatoarivony I, Villeret R, Rodhain F, Duchemin JB, et al. Population genetic structure and competence as a vector for dengue type 2 virus of Aedes aegypti and Aedes albopictus from Madagascar. Am J Tropical Med Hygiene 2001;65:491–7. https://doi.org/10.4269/ajtmh.2001.65.491.

[37] Barrera R, Amador M, MacKay AJ. Population dynamics of Aedes aegypti and dengue as influenced by weather and human behavior in San Juan, Puerto Rico. PLoS Neglected Tropical Dis 2011;5:e1378. https://doi.org/10.1371/journal. pntd.0001378.

[38] V. Duong L. Lambrechts R.E. Paul S. Ly R.S. Lay K.C. Long et al. Asymptomatic humans transmit dengue virus to mosquitoes Proceedings of the National Academy

of Sciences of the United States of America. 112 2015 14688 14693 (10.1073/pnas.1508114112).

[39] Bartley LM, Donnelly CA, Garnett GP. The seasonal pattern of dengue in endemic areas: mathematical models of mechanisms. Trans R Soc Trop Med Hyg 2002;96: 387–97. https://doi.org/10.1016/s0035-9203(02)90371-8.

[40] Kim JE, Lee H, Lee CH, Lee S. Assessment of optimal strategies in a two-patch dengue transmission model with seasonality. PloS one 2017;12:e0173673. https://doi.org/10.1371/journal.pone.0173673.

[41] Polwiang S. The time series seasonal patterns of dengue fever and associated weather variables in Bangkok (2003-2017). BMC Infectious Dis 2020;20:208. https://doi.org/10.1186/s12879-020-4902-6.

[42] Teurlai M, Huy R, Cazelles B, Duboz R, Baehr C, Vong S. Can human movements explain heterogeneous propagation of dengue fever in Cambodia? PLoS Neglected Tropical Dis 2012;6:e1957. https://doi.org/10.1371/journal.pntd.0001957.

[43] Mordecai EA, Cohen JM, Evans MV, Gudapati P, Johnson LR, Lippi CA, Miazgowicz K, Murdock CC, Rohr JR, Ryan SJ, et al. Detecting the impact of temperature on transmission of Zika, dengue, and chikungunya using mechanistic models. PLoS Neglected Tropical Dis 2017;11:e0005568. https://doi.org/10.1371/journal.pntd.0005568.

[44] Lai S, Johansson MA, Yin W, Wardrop NA, van Panhuis WG., Wesolowski A, et al. Seasonal and interannual risks of dengue introduction from South-East Asia into China, 2005-2015. PLoS neglected tropical diseases 2018. 12, e0006743. doi: 10.1371/journal.pntd.0006743.

[45] Joanne S, Vythilingam I, Teoh BT, Leong CS, Tan KK, Wong ML, Yugavathy N, AbuBakar S. Vector competence of Malaysian Aedes albopictus with and without Wolbachia to four dengue virus serotypes. Tropical medicine & international health. 2017. 22, 1154-1165. doi:10.1111/tmi.12918.

[46] Tran A, L'Ambert G, Lacour G, Benoit R, Demarchi M, Cros M, Cailly P, Aubry-Kientz M, Balenghien T, Ezanno P. A rainfall- and temperature-driven abundance model for Aedes albopictus populations. International journal of environmental research and public health. 2013 10, 1698-1719. doi:10.3390/ijerph10051698.

[47] Cailly P, Tran A, Balenghien T, L'Ambert G, Toty C, Ezanno P. A climate-driven abundance model to assess mosquito control strategies. Ecol Model. 2012 227, 7-17. doi:10.1016/j.ecolmodel.2011.10.027.

[48] Ezanno P, Aubry-Kientz M, Arnoux S, Cailly P, L'Ambert G, Toty C, Balenghien T, Tran A. A generic weather-driven model to predict mosquito population dynamics applied to species of Anopheles, Culex and Aedes genera of southern France. Preventive veterinary medicine. 2015. 120, 39-50. doi:10.1016/j.prevetmed.2014.12.018.

[49] Pandey A, Mubayi A, Medlock J. Comparing vector-host and SIR models for dengue transmission. Mathematical biosciences. 2013. 246, 252-259. doi:10.1016/j.mbs.2013.10.007.

[50] Gubler DJ, Suharyono W, Tan R, Abidin M, Sie A. Viraemia in patients with naturally acquired dengue infection. Bull World Health Organ 1981;59:623–30.

[51] Iyaloo DP, Degenne P, Elahee KB, Seen DL, Bheecarry A, & Tran A. ALBOMAURICE: A predictive model for mapping Aedes albopictus mosquito populations in Mauritius. SoftwareX, 13, 100638.

[52] Aliyu AI, Inc M, Yusuf A, Baleanu D. A fractional model of vertical transmission and cure of vector-borne diseases pertaining to the Atangana-Baleanu fractional derivatives. Chaos, Solitons Fractals 2018;116:268–77.

[53] Amann H. Ordinary differential equations: an introduction to nonlinear analysis. Walter de Gruyter; 2011.

[54] Chicone C. Ordinary differential equations with applications. Springer Science & Business Media; 2006.